

**Manuscript version: Author's Accepted Manuscript**

The version presented in WRAP is the author's accepted manuscript and may differ from the published version or Version of Record.

**Persistent WRAP URL:**

<http://wrap.warwick.ac.uk/117270>

**How to cite:**

Please refer to published version for the most recent bibliographic citation information. If a published version is known of, the repository item page linked to above, will contain details on accessing it.

**Copyright and reuse:**

The Warwick Research Archive Portal (WRAP) makes this work by researchers of the University of Warwick available open access under the following conditions.

Copyright © and all moral rights to the version of the paper presented here belong to the individual author(s) and/or other copyright owners. To the extent reasonable and practicable the material made available in WRAP has been checked for eligibility before being made available.

Copies of full items can be used for personal research or study, educational, or not-for-profit purposes without prior permission or charge. Provided that the authors, title and full bibliographic details are credited, a hyperlink and/or URL is given for the original metadata page and the content is not changed in any way.

**Publisher's statement:**

Please refer to the repository item page, publisher's statement section, for further information.

For more information, please contact the WRAP Team at: [wrap@warwick.ac.uk](mailto:wrap@warwick.ac.uk).

# A Tuning Method of Active Disturbance Rejection Control for a Class of High-order Processes

Ting He, Zhenlong Wu, Donghai Li and Jihong Wang, *Senior Member IEEE*

**Abstract**—This paper aims to propose a quantitative tuning method for active disturbance rejection control (ADRC) that controls the  $K(Ts+1)^n$ -type high-order processes. An asymptote in the Nyquist curve has been observed for the first time and its mathematical expression has been deduced. An asymptote condition is provided in order to derive a parameter tuning rule under the sensitivity constraint. Although this proposed tuning rule is originally designed for a certain type of high-order processes, it can be extended to other types processes that can be approximated into the form of  $K(Ts+1)^n$ . Comparisons with different PID control strategies have been conducted for a range of cases to demonstrate the efficiency of the proposed tuning method. Finally, the effectiveness of the proposed tuning rule is experimentally verified on water tank system that exhibits high-order dynamics. Field tests on the superheater steam temperature control of a circulating fluidized bed (CFB) power plant further demonstrate its potential for applications in complex industrial processes.

**Index Terms**—Active Disturbance Rejection Control, high-order processes, parameter tuning, steam temperature control, maximum sensitivity.

## I. INTRODUCTION

High-order systems represent a common feature existing in many industrial processes, such as the superheater steam temperature and main steam pressure control in power plants [1][2][3]. In fact, many complex industrial processes with nonlinear dynamics are inherently of high-order [4]. Transfer function approximation for a distributed parameter system often results in a high-order model representation [5]. However, designing high-order controllers for high-order processes brings complexities in control analysis, control algorithm implementation and parameter tuning. Therefore, in industrial practice, lower order controllers are usually preferred. For instance, it is reported that more than 94% of the controllers configured in power plant in Guangdong province, China, are lower order PI controllers [6]. When the low order controller is

used, higher-order dynamics are often considered as a part of the internal disturbances. Besides, various external disturbances and uncertainties are inevitable in industrial processes, such as variation in fuel quality, load change, environmental temperature and pressure changes. Conventional PI/PID controllers are found inadequate in dealing with all kind of disturbances in many cases, thus efficient anti-disturbance techniques need to be applied in industrial control [7].

Active disturbance rejection control (ADRC) is one of the notable disturbance/uncertainty estimation and attenuation techniques [8]. ADRC is firstly proposed by Han [9] to serve as an alternative control to the classical PID [10]. The extended state observer (ESO), the core part of ADRC, estimates the internal uncertainties (the un-modeled dynamics, the higher-order dynamics, and parameter errors) and the external disturbances as a lumped term called the total disturbance, which is then compensated via control actions in real time. During the last two decades, ADRC has been extensively investigated and applied by many researchers in different countries and in different industrial sectors [11]. The theoretical analysis of ADRC with regard to convergence and stability proof have been studied in [12][13]. Performance and properties of ADRC have been analyzed in frequency domain [14]. Improved ADRC have been proposed to address the challenges caused by large time-delays [15], non-minimum phase [16], and multi-variable coupling [17][18]. ADRC were initially studied via simulations and experiments and then extended to industrial applications with the range from motion control [19], electronic and mechanical systems [20] to process control [21].

Control parameter tuning is a key factor for ADRC's successful implementation in real industrial processes. However, there are no well-established quantitative tuning rules for ADRC parameters, especially for high-order processes. Most of the tuning work is performed manually, although the process of trial and error is tedious, and in some cases, frustrating. There are successful attempts using heuristic algorithms to optimize parameters [2][22], but the tuning process is time-consuming and not convenient enough for industrial sectors to adopt. An important progress was made by Gao [23] in 2006. The bandwidth-parameterization in [23] had greatly simplified the tuning process by reducing six tuning parameters to three. Chen [24] graphically presented the stable region of second-order ADRC parameters and refined the tuning process in the sight of closed loop desired dynamics. Wang [25] proposed a particular ADRC tuning method for time-delay systems. However, those studies on parameter

Manuscript received June 03, 2018; revised October 07, 2018 and January 30, 2019; accepted March 08, 2019. This work was supported by the National Key Research and Development Program of China, 2016YFB0901405 and the National Natural Science Foundation of China, 51876096. (*Corresponding author: Donghai Li.*)

T. He, Z. Wu and D. Li are with the State Key Lab of Power Systems, Department of Energy and Power Engineering, University of Tsinghua, Beijing 100084, China (e-mail: he-t14@mails.tsinghua.edu.cn; wu-zl15@mails.tsinghua.edu.cn; lidongh@mail.tsinghua.edu.cn).

J. Wang is with the School of Engineering, University of Warwick, Coventry CV4 7AL, U.K. (e-mail: jihong.wang@warwick.ac.uk).



$$G_l(s) = G_p G_c F = \frac{(k_p \beta_1 + k_d \beta_2 + \beta_3)s^2 + (k_p \beta_2 + k_d \beta_3)s + k_p \beta_3}{b_0 [s^3 + (\beta_1 + k_d)s^2 + (\beta_2 + k_d \beta_1 + k_p)s]} \frac{K}{(Ts+1)^n} \quad (8)$$

$$G_{cl}(s) = \frac{G_p G_c}{1 + G_p G_c F} = \frac{k_p C(s) K}{b_0 A(s) (Ts+1)^n + KB(s)} \quad (9)$$

$$A(s) = s^3 + (\beta_1 + k_d)s^2 + (\beta_2 + k_d \beta_1 + k_p)s$$

$$B(s) = (k_p \beta_1 + k_d \beta_2 + \beta_3)s^2 + (k_p \beta_2 + k_d \beta_3)s + k_p \beta_3$$

$$C(s) = s^3 + \beta_1 s^2 + \beta_2 s + \beta_3$$

Thus, the frequency characteristic of the open loop transfer function..is

$$G_l(i\omega) = G_c(i\omega)G_p(i\omega)F(i\omega)$$

$$= \frac{k_p \beta_3 - (k_p \beta_1 + k_d \beta_2 + \beta_3)\omega^2 + (k_p \beta_2 + k_d \beta_3)\omega i}{-(\beta_1 + k_d)\omega^2 + [(\beta_2 + k_d \beta_1 + k_p)\omega - \omega^3]i} \frac{K}{b_0 (T\omega i + 1)^n} \quad (10)$$

Figure 3 shows the Nyquist diagram of  $G_l(i\omega)$ . Combined with equation (6), the definition of the maximum sensitivity  $M_s$  can be graphically interpreted:  $M_s$  equals to the inverse of the shortest distance between the Nyquist curve of  $G_l(i\omega)$  and the critical point  $(-1,0i)$ .

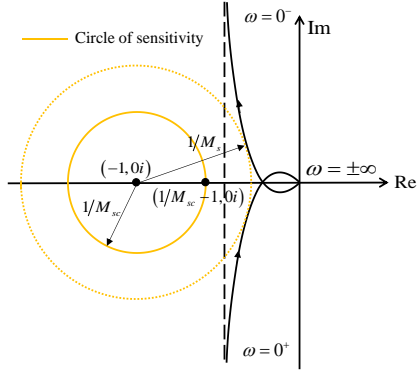


Fig. 3. Graphical interpretation of maximum sensitivity  $M_s$ .

Given a certain maximum sensitivity constraint  $M_{sc}$ , a circle of sensitivity, centered at  $(-1,0i)$  with the radius  $1/M_{sc}$ , can be constructed. Then the actual value of the maximum sensitivity  $M_s$  is guaranteed to be not higher than  $M_{sc}$ , provided that the Nyquist curve of  $G_l(i\omega)$  does not enter into the circle of sensitivity. This important principle will be used in next subsection to derive ADRC parameters tuning rules.

### B. Derivation of ADRC tuning rule

As it is mentioned in Section II,  $\omega_c$  is called the desired closed-loop bandwidth, also, the desired closed-loop system poles. When the observer gains are properly chosen so that the ESO states  $z_1, z_2$  and  $z_3$  track  $y, \dot{y}$  and  $f$  well, combining equations (3), (4), the second equation in (1) can be rewritten as

$$\ddot{y} \approx f + b_0 \frac{[k_p(r-y) - k_d \dot{y}] - f}{b_0} = k_p(r-y) - k_d \dot{y}. \quad (11)$$

Therefore, the transfer function from the reference  $r$  to the output  $y$  can be approximated into

$$G_{yr}(s) = \frac{R(s)}{Y(s)} \approx \frac{k_p}{s^2 + k_d s + k_p} = \frac{\omega_c^2}{(s + \omega_c)^2}. \quad (12)$$

The choice of  $\omega_c$  mainly influences the set-point tracking performance. In [24], it is recommended that  $\omega_c = 10/t_s^*$ , where  $t_s^*$  is the desired settling time. The choice of the desired settling

time  $t_s^*$  can incorporate the information of the process model. In this study, the controlled process,  $K/(Ts+1)^n$ , can be seen as  $n$  first-order processes  $1/(Ts+1)$  being cascaded connecting together. Since parameters  $n$  and  $T$  influence the transient time of the process most, it is natural to assume that  $t_s^*$  is proportional to  $nT$ . Therefore,  $\omega_c$  is decided as

$$\omega_c = 10/knT, \quad (13)$$

where  $k$  is the desired settling time factor and it is the only tuning parameter in this proposed tuning method.

Bandwidth  $\omega_o$  is the ESO pole. In general, a larger  $\omega_o$  value can speed up the total disturbance being estimated and rejected, so a large  $\omega_o$  is usually preferred. However, in practice, the sampling rate limits the upper bound of  $\omega_o$ . In general, it is recommended that [23]

$$\omega_o = 10\omega_c. \quad (14)$$

The tuning equation of  $\omega_c$  is derived from the perspective of the desired set-point tracking, and the choice of  $\omega_o$  considers the disturbance rejection speed. Now, the design of  $b_0$  will consider the closed-loop system robustness, that is, sensitivity constraint will be applied in determination of  $b_0$ .

Using the bandwidth-parameterization (5) and equation (14), the frequency characteristics of the open loop system transfer function  $G_l(i\omega)$ , equation (10), can be rewritten as

$$G_l(i\omega) = \frac{(\omega_c^2/\omega - 1.63\omega) + 2.3\omega_c i}{-32\omega_c \omega + (361\omega_c^2 - \omega^2)i} \times \frac{1}{(1+T\omega i)^n} \frac{10^3 \omega_c^3 K}{b_0}. \quad (15)$$

When come to derive PID control parameters under the sensitivity constraints, previous studies [26][27] have made effort on solving the nonlinear equations related to the definition of maximum sensitivity and the open loop transfer function. It is possible to yield explicit solutions for PID design, although derivation operation and numerical calculation are often involved, making it not easy for control engineers to execute the solving procedure. For the ADRC control system studied in this work, it is very difficult to directly solve the sensitivity constraint from equations (6) and (15). It is highly nonlinear because of the absolute operation. In addition, it is at least 5th-degree, which means it almost impossible to obtain an explicit solution.

Instead of strictly solving the sensitivity constraint, an alternative asymptote constraint is used to determine  $b_0$  in this study. The asymptote is vertical to the real axis in the Nyquist plot of  $G_l(i\omega)$  (see Fig. 3). Considering the relationship between the asymptote and the circle of sensitivity, an asymptote condition is further proposed below:

Provided that the vertical asymptote of Nyquist curve  $G_l(i\omega)$  is located at the right side of the circle of sensitivity, and the Nyquist curve of  $G_l(i\omega)$  does not enter into the circle of sensitivity, then the actual maximum sensitivity  $M_s$  is guaranteed to be smaller than  $M_{sc}$ .

The asymptote function of Nyquist curve  $G_l(i\omega)$  needs to be found. Let  $x, y$  denote the real axis and imagine axis respectively, so  $G_l(i\omega) = x(\omega) + y(\omega)i$ . The line  $x = a$  is a vertical asymptote of the plot of  $G_l(i\omega)$ , when there exists a  $\omega = \omega^*$  so that

$$\begin{cases} \lim_{\omega \rightarrow \omega^*} x(\omega) = \lim_{\omega \rightarrow \omega^*} \operatorname{Re}[G_l(i\omega)] = a \\ \lim_{\omega \rightarrow \omega^*} y(\omega) = \lim_{\omega \rightarrow \omega^*} \operatorname{Im}[G_l(i\omega)] = \pm\infty. \end{cases} \quad (16)$$

Observed from Fig. 3, the imaginary coordinate of the Nyquist curve tends to infinity when  $\omega \rightarrow \pm 0$ , so the limiting values of the real and imaginary part of  $G_l(i\omega)$  are concerned when  $\omega \rightarrow \pm 0$ . Let

$$(1 + T\omega i)^n = p_1 + p_2 i, \quad (17)$$

then

$$\begin{aligned} p_1 &= 1 + C_n^2 (T\omega)^2 (-1)^1 + C_n^4 (T\omega)^4 (-1)^2 + \dots \\ p_2 &= nT\omega + C_n^3 (T\omega)^3 (-1)^1 + C_n^5 (T\omega)^5 (-1)^2 + \dots \end{aligned} \quad (18)$$

Therefore, we have

$$G_l(i\omega) = \frac{[(798.3\omega_c^3 + 49.86\omega_c\omega^2) - (361\omega_c^4/\omega - 515.83\omega_c^2\omega + 1.63\omega^3)i]}{[(-32\omega_c\omega)^2 + (361\omega_c^2 - \omega^2)^2]} \quad (19)$$

$$\times \frac{(p_1 - p_2 i) 10^3 \omega_c^3 K}{(p_1^2 + p_2^2) b_0}.$$

Then,

$$\operatorname{Re}[G_l(i\omega)] = \frac{(798.3\omega_c^3 + 49.86\omega_c\omega^2)p_1 - (361\omega_c^4/\omega - 515.83\omega_c^2\omega + 1.63\omega^3)p_2}{[(-32\omega_c\omega)^2 + (361\omega_c^2 - \omega^2)^2]} \quad (20)$$

$$\operatorname{Im}[G_l(i\omega)] = \frac{10^3 \omega_c^3 K}{(p_1^2 + p_2^2) b_0} \times \frac{- (798.3\omega_c^3 + 49.86\omega_c\omega^2)p_2 - (361\omega_c^4/\omega - 515.83\omega_c^2\omega + 1.63\omega^3)p_1}{[(-32\omega_c\omega)^2 + (361\omega_c^2 - \omega^2)^2]} \quad (21)$$

When  $\omega \rightarrow 0^+$ ,  $p_1 \rightarrow 1$ ,  $p_2 \rightarrow nT\omega$ , and  $p_1^2 + p_2^2 = |1 + T\omega i|^2 \rightarrow 1$ , in the expressions of  $\operatorname{Re}[G_l(i\omega)]$  and  $\operatorname{Im}[G_l(i\omega)]$ , the terms in the form of multiplying  $\omega$  diminish to 0, while the terms which are divided by  $\omega$  tend to  $\infty$ . Thus, we have

$$\begin{aligned} \lim_{\omega \rightarrow 0^+} \operatorname{Re}[G_l(i\omega)] &= \frac{(798.3\omega_c^3) - (361nT\omega_c^4)}{361^2 \omega_c^4} \times \frac{10^3 \omega_c^3 K}{b_0} \\ &= (6.1256\omega_c^2 - 2.77\omega_c^3 nT) K / b_0 \end{aligned} \quad (22)$$

$$\lim_{\omega \rightarrow 0^+} \operatorname{Im}[G_l(i\omega)] = +\infty.$$

As previously, when  $\omega \rightarrow 0^+$ ,

$$\lim_{\omega \rightarrow 0^+} \operatorname{Re}[G_l(i\omega)] = (6.1256\omega_c^2 - 2.77\omega_c^3 nT) K / b_0 \quad (23)$$

$$\lim_{\omega \rightarrow 0^+} \operatorname{Im}[G_l(i\omega)] = -\infty.$$

Equations (22) and (23) show that there exists  $\omega^* = 0$  satisfying the definition in (16), so the function of the asymptote is

$$x = (6.1256\omega_c^2 - 2.77\omega_c^3 nT) K / b_0. \quad (24)$$

As it is shown in the Fig. 3, the right endpoint of the circle of sensitivity locates at  $(1/M_{sc} - 1, 0i)$ . Applying the asymptote condition,

$$(6.1256\omega_c^2 - 2.77\omega_c^3 nT) K / b_0 > 1/M_{sc} - 1, \quad (25)$$

and solving (25) for  $b_0$ , we have

$$b_0 > (2.77\omega_c nT - 6.1256)\omega_c^2 K M_{sc} / (M_{sc} - 1) \quad (26)$$

Since increasing  $b_0$  can reduce the maximum sensitivity  $M_s$ , for a conservative design, let  $b_0$  be  $m$  times the lower limit. Then, the parameter  $b_0$  can be determined by

$$b_0 = m(2.77\omega_c nT - 6.1256)\omega_c^2 K M_{sc} / (M_{sc} - 1). \quad (27)$$

Coefficient  $m$  and  $M_{sc}$  can be chosen according to engineering experience. In this study, we choose  $m = 1.4$ , and the maximum sensitivity constraint  $M_{sc}$  is chosen as the maximum of the allowable value, 2.5, thus (27) becomes

$$b_0 = (6.4541\omega_c nT - 14.2726)\omega_c^2 K. \quad (28)$$

In summary, the tuning rules for the second-order linear ADRC controlling high-order processes  $K/(Ts+1)^n$  are as follow:

$$\begin{cases} \omega_c = 10/knT \\ \omega_o = 10\omega_c \\ b_0 = (6.4541\omega_c nT - 14.2726)\omega_c^2 K. \end{cases} \quad (29)$$

Similarly, the tuning rules for the first-order linear ADRC can also be derived.

$$\begin{cases} \omega_c = 10/knT \\ \omega_o = 10\omega_c \\ b_0 = (11.1111nT\omega_c - 12.8042)\omega_c^2 K \end{cases} \quad (30)$$

**Remark:** Applying the proposed second-order ADRC tuning method to the high-order process, two interesting conclusions can be further inferred.

1) The asymptotes for the different controlled systems are the same. Substitute the expression of  $b_0$ , equation (28), into the asymptote function (24), then we get  $x = -0.429$ .

It shows the real axis value of the asymptote remains constant, which can be verified in the Fig. 4(b). Different Nyquist curves of  $G_l(i\omega)$  converge to the same asymptote.

2) Complementary maximum sensitivity  $M_t \leq 1$ .

Complementary maximum sensitivity  $M_t$  is also an important indicator for measuring robustness. It implies the sensitivity of the closed-loop system to the large process dynamic variations.  $M_t$  is defined as

$$M_t = \max_{\omega} |G_l(i\omega)/(1 + G_l(i\omega))| \quad \omega \in (-\infty, +\infty). \quad (31)$$

Since  $G_l(i\omega) = x(\omega) + y(\omega)i$ ,

$$M_t = \max_{\omega} \sqrt{\frac{x(\omega)^2 + y(\omega)^2}{1 + 2x(\omega) + x(\omega)^2 + y(\omega)^2}}, \quad (32)$$

if  $x(\omega) \geq -0.5$ ,  $M_t \leq 1$ . The proposed ADRC tuning method gives asymptote function  $x = -0.429$ . Under the proposed tuning method, the Nyquist curve of  $G_l(i\omega)$  can be tuned to be located at the right side of the asymptote line, that is,  $x(\omega)$  is not smaller than -0.429. Therefore,  $M_t \leq 1$  is achieved. This conclusion indicates that the proposed ADRC tuning method derived under  $M_s$  constraint can lead to satisfactory  $M_t$ .

### C. Tuning parameter

The effect of the tuning parameter  $k$  should be clear to users. According to [28], to ensure the closed loop system stability,  $b_0$  and the process gain  $K$  must share the same sign. Then, the upper limit of the desired settling time factor  $k$  can be deducted from (28),  $0 < k < 4.5$ . In order to avoid unstable or oscillatory

output response caused by nearing the critical values, the range of the tuning parameter  $k$  can be further narrowed. In engineering practice, the range of  $k = 1.0 \sim 4.0$  is suitable for most high-order process. However, the adjustment of  $k$  is still necessary to achieve a certain robustness level. Consider a cascaded fifth-order process

$$G_p = 1/(8s+1)^5. \quad (33)$$

The model parameter  $n = 5$ ,  $T = 8$ , and  $K = 1$  can be directly used to calculate the ADRC parameters by (29). The control results and robustness indices under the different tuning parameter  $k$  are shown in Fig. 4. In general, increasing  $k$  results in faster tracking response and better disturbance rejection performance, but higher maximum sensitivity  $M_s$ . This influence pattern can be used as a crude guideline to adjust  $k$  to a certain maximum sensitivity  $M_s$ .

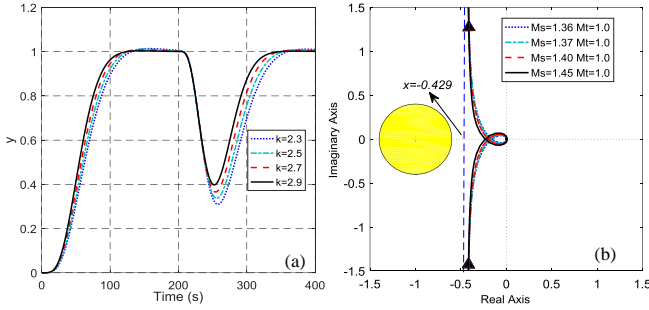


Fig. 4. Performance and robustness under different tuning parameter  $k$ . (a) tracking response ( $t=0-200$  s) and disturbance rejection ( $t=200-400$  s) of  $G_p$ ; (b) Nyquist diagram and robustness indices of  $G_p$ .

Although this study provides a simple straightforward tuning method for ADRC parameters, sometimes it is better to give the values of parameters in the form of limitations. If a range of the tuning parameter  $k$  is decided, then the ADRC parameters can be presented in the form of limitations. For example, if an appropriate range of  $k$  is tuned for a certain process,  $k = [k^-, k^+]$ , then the ranges of ADRC parameters are

$$\begin{cases} \omega_c = \left[ \frac{10}{k^+ n T}, \frac{10}{k^- n T} \right] \\ \omega_o = \left[ \frac{100}{k^+ n T}, \frac{100}{k^- n T} \right] \\ b_o = \left[ \left( \frac{6454.1}{k^{+3}} - \frac{1427.26}{k^+} \right) \frac{K}{n^2 T^2}, \left( \frac{6454.1}{k^{-3}} - \frac{1427.26}{k^-} \right) \frac{K}{n^2 T^2} \right] \end{cases} \quad (34)$$

**Theorem 1:** Assuming the process is modelled by  $K/(Ts+1)^n$ , and the second-order ADRC is given by (2)~(4). ADRC parameters  $\omega_c$ ,  $\omega_o$  and  $b_o$  are controller parameters that need to be determined. Then, we have the following results:

- i) There exists an asymptote of the Nyquist curve of the open-loop transfer function (8), which can be described by (24).
- ii) If the asymptote is located at the right side of the circle of sensitivity, which is constructed by maximum sensitivity constraint  $M_{sc}$ . Then  $b_o$  satisfies the inequality (26) and  $b_o$  can be  $m$  times the lower limit, i.e.,  $b_o$  can be given by the equality (27).
- iii) ADRC parameters  $\omega_c$ ,  $\omega_o$  are given by (13) and (14), where the only tuning parameter  $k$  satisfies  $0 < k < 4.5$ , so that ADRC can be tuned to achieve satisfactory performance

and robustness.

**Remark 1:**  $m$  and  $M_{sc}$  in the Theorem can be determined by engineering experience. In this study, we choose  $m = 1.4$ ,  $M_{sc} = 2.5$ , then  $\omega_c$ ,  $\omega_o$  and  $b_o$  can be given by (29).

**Remark 2:** Similarly, when the controller is first-order ADRC, the controller parameters  $\omega_c$ ,  $\omega_o$  and  $b_o$  can be given by (30), where the only tuning parameter  $k$  satisfies  $0 < k < 8.6$ .

**Remark 3:** For self-regulatory processes which can be approximated into  $K/(Ts+1)^n$ , the ADRC tuning equations (29) and (30) can also be applied.

#### IV. ILLUSTRATIVE EXAMPLES

In order to demonstrate the efficacy of the proposed ADRC tuning method, comparative simulation studies have been carried out for different types of processes.

##### A. Approximation method

Although the proposed ADRC tuning method is originally designed for the certain type of high-order processes,  $K/(Ts+1)^n$ , the proposed ADRC tuning method can also be applied to other types of processes, which can be approximated into the form of  $K/(Ts+1)^n$ . The empirical two-point method is used for model approximation or process identification [29]. The principle of the two-point approximation is illustrated in Fig. 5 and (35). If the open-loop system step response indicates that the process is self-regulating, find the time coordinates  $t_1$ ,  $t_2$  corresponding to  $0.4y(\infty)$  and  $0.8y(\infty)$ . When  $t_1/t_2 \geq 0.46$  the process can be approximated to the high order process. Applying the empirical formulas (35), the model parameters  $n$ ,  $T$  and  $K$  can therefore be determined. It should be pointed out that the order  $n$  should be rounded to an integer in the calculation.

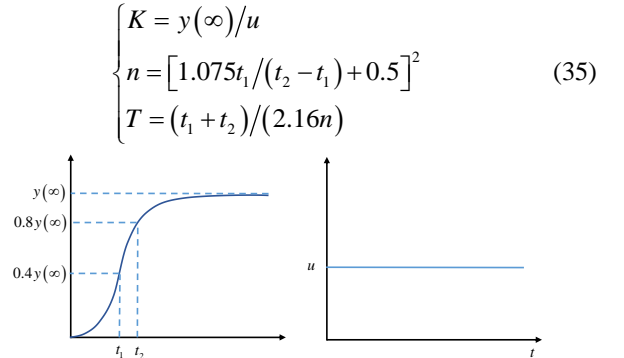


Fig. 5. Two-point approximation method

##### B. Simulation examples

**Example 1:** 100<sup>th</sup>-order process

$$G_{p1} = 1/(s+1)^{100} \quad (36)$$

This is an extreme case of a standard  $K/(Ts+1)^n$  - type high-order process. The model parameters  $n=100$ ,  $T=1$ , and  $K=1$  can be directly used for ADRC parameters calculation. The well-known Skogestad IMC (SIMC) [30] and the  $M_s$ -constrained integral gain optimization (MIGO) [26] design methods are also applied to the process  $G_{p1}$  for comparison. Since performance and robustness are a pair of ever-lasting paradox, for fair comparison, the maximum sensitivity  $M_s$  is tuned to have the same value. Note that the MIGO method

instead of the simpler tuning rule AMIGO [31] is used in the simulations because the AMIGO does not have a tuning parameter to achieve a desired maximum sensitivity. Therefore, the tracking performance, disturbance rejection ability, and the control effort of different tuning methods can be compared under the same robustness level. The output responses with a unit load disturbance added to the system at  $t = 800$  s are depicted in Fig. 6(a). The simulation step size is  $h = 0.01$ . For the three simulations, white noises with a variance of 0.005 are added during the last one third of the simulation time span  $t_E$ . The parameters setting and performance indices are summarized in Table 1, including robustness indices  $M_s, M_t$ , output performance settling time  $T_s$ , overshoot  $\sigma$ , variance of control input noise  $\sigma_n$ , the integrated time-weighted absolute error (ITAE), and the control effort index total variation (TV) of the input. Indices ITAE and TV are defined in (37). They should be as small as possible [30].

$$\text{ITAE} = \int_0^{2/3t_E} t |r(t) - y(t)| dt \quad \text{TV} = \sum_{i=1}^{2/3t_E/h} |u_{i+1} - u_i| \quad (37)$$

It can be seen from the comparative results that under the same robustness level  $M_s = 1.51$ , the proposed ADRC tuning rule provides smooth and non-overshoot tracking, meanwhile, gives better performance in disturbance rejection among these three control design methods. Moreover, it handles measurement well without additional filter. This 100<sup>th</sup>-order

process behaves like systems with large time-delay. The success of controlling this model implies the possibility of applying this tuning method to other delay-dominant processes.

**Example 2:** Oscillatory high-order process

$$G_{p2} = \frac{9}{(s+1)(s^2+2s+9)} \approx \frac{1}{(0.2755s+1)^4}. \quad (38)$$

This is a non- $K/(Ts+1)^n$ -type high-order process.  $G_{p2}$  can be approximated to a fourth-order process by using equations (35) of the two-point approximation method. Although the approximated high-order process cannot capture the oscillatory feature of the original process, the ability of ADRC estimating and compensating the un-modelled dynamics enables high-order process based ADRC design to provide good control results on oscillatory process. The proposed tuning equations (29) can be used to decide ADRC parameters. For SIMC-PID tuning, process  $G_{p2}$  is approximated to a second-order plus time delay process,  $e^{-0.34s}/((0.72s+1)(0.14s+1))$ . ADRC, SIMC-PID and MIGO are tuned to have the same maximum sensitivity, which is  $M_s = 1.86$ . The detailed parameter settings and the control results are show in Table I and Fig. 6(b).

It can be seen from the Fig. 6(b) and Table 1 that the proposed ADRC tuning method provides least-oscillatory tracking performance with small overshoot, and the noise level under ADRC control is acceptable.

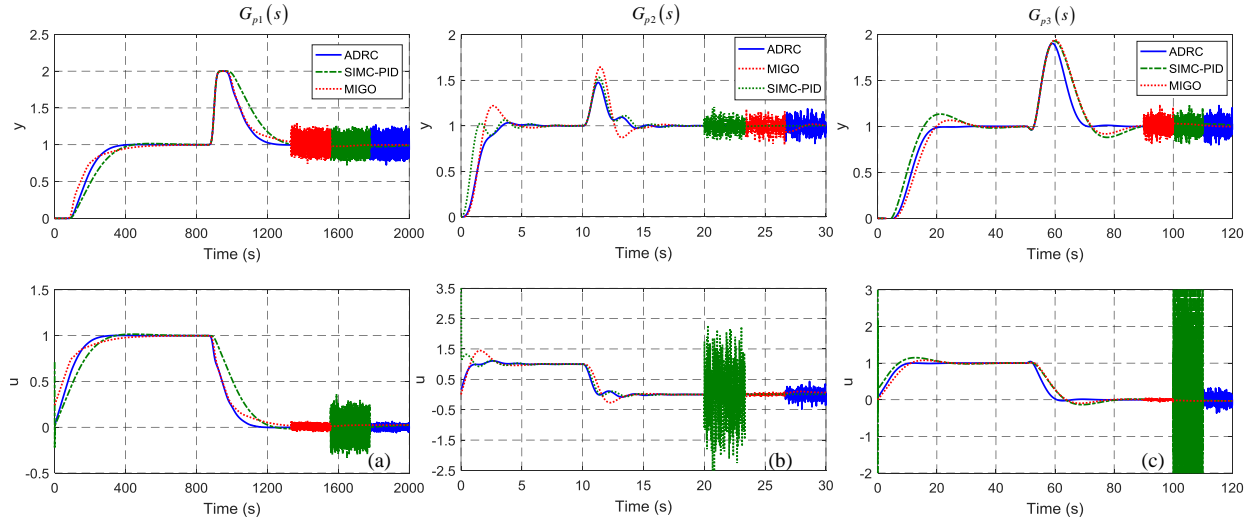


Fig. 6. Response comparison under different control strategies

TABLE I  
CONTROLLER PARAMETERS AND PERFORMANCE INDICES FOR  $G_{p1}(s)$ ,  $G_{p2}(s)$ , AND  $G_{p3}(s)$

Models	Method	Tuning parameter	Controller parameters	$M_s$	$M_t$	Tracking		Disturbance rejection		ITAE	TV	$\sigma_n$
						$T_s/s$	$\sigma/\%$	$T_s/s$	$\sigma/\%$			
$G_{p1}(s)$	ADRC	$k=1.5$	$\omega_c=0.067, \omega_o=0.667, b_o=0.128$	1.51	1.00	349	0.24	415	98.6	206306	1.98	0.0003
	SIMC-PID	$\tau_c=1.2\theta$	$K_p=0.833, K_i=0.333, K_d=0.500$	1.51	1.00	413	1.23	520	101.4	302058	3.45	0.0076
	MIGO	$M_s=1.5$	$K=0.2406, K_i=0.204, b=1$	1.51	1.00	496	0.25	578	99.9	239575	1.76	0.0003
$G_{p2}(s)$	ADRC	$k=3.34$	$\omega_c=2.717, \omega_o=27.17, b_o=37.34$	1.86	1.08	4.41	3.38	4.65	47.5	13.8	2.64	0.0021
	SIMC-PID	$\tau_c=1.35\theta$	$K_p=1.069, K_i=1.242, K_d=0.124$	1.86	1.03	5.83	6.43	4.88	53.3	15.5	15.0	1.0052
	MIGO	$M_s=1.86$	$K=0.456, K_i=1.414, b=0$	1.86	1.29	6.13	22.0	5.16	64.5	19.9	3.58	0.0008
$G_{p3}(s)$	ADRC	$k=2.55$	$\omega_c=0.509, \omega_o=5.088, b_o=2.86$	1.80	1.00	19.3	0.11	21.6	90.2	651	2.12	0.0016
	SIMC-PID	$\tau_c=0.6\theta$	$K_p=0.284, K_i=0.114, K_d=0.171$	1.80	1.11	31.6	14.0	39.3	92.6	951	36.5	4.7022
	MIGO	$M_s=1.8$	$K=0.304, K_i=0.106, b=0$	1.80	1.04	31.6	6.87	36.8	93.4	926	2.43	0.0005

**Example 3:** Process with time delay, non-minimum phase and high order

$$G_{p3} = \frac{(-s+1)e^{-2s}}{(s+1)^5} \approx \frac{1}{(0.5929s+1)^{13}} \quad (39)$$

As previously, process  $G_{p3}$  is approximated to a 13<sup>th</sup>-order process. Then, the proposed ADRC tuning method is applied and the SIMC-PID and MIGO are also performed for comparison. The comparative results in Fig. 6(c) and Table I show that the proposed ADRC tuning method delivers smooth and non-overshoot set-point tracking performance, better performance in disturbance rejection, while it requires least TV in control input.

Three illustrative examples have shown that the proposed ADRC tuning method is capable of providing good performance for cascade high-order process, non-cascade high-order process, time-delay process and non-minimum phase process. More simulation results can be found in *Supplementary materials*.

### Discussion:

The application scope of the proposed ADRC tuning method should be discussed. Generally speaking, the proposed tuning method is applicable to processes that can be modelled as or approximated to the form of  $K/(Ts+1)^n$ . The process must be self-regulatory, so processes with unstable or integrating characteristics are beyond the scope of this study. Processes with delay, oscillatory and non-minimum phase characteristics are target processes for the proposed tuning method. To be more specific, based on extensive simulations, delay-dominated systems, whose delay-lag constant ratio  $\tau/T > 1$ , are highly likely to be approximated to  $K/(Ts+1)^n$ . Oscillatory systems with the damping ratio not smaller than 0.3, and non-minimum phase system with inverse overshoot not exceeding 30% of the steady-state gain are also recommended for this proposed tuning method. Since most of the industrial processes are self-regulatory, and many processes can be modelled into this high-order form, such as the steam temperature and pressure control, combustion control system in power plant, we believe that the proposed method is of certain generality and practical value.

The proposed tuning method requires the value of model parameters  $K, n, T$ , but this does not mean the proposed ADRC tuning laws depend on the exact modelling of the actual processes. Simulation examples of  $G_{p2}$  and  $G_{p3}$  show that a rough approximation to the original process is enough for ADRC design. In addition, when a process is identified or approximated to a  $K/(Ts+1)^n$ -type model, different choices of the model order  $n$  do not influence the control results notably. For instance, when the 100<sup>th</sup>-order process  $G_{p1}$ , is modelled with different order  $n$ , such as  $n=102, 98, 70$ , the control results based on these models with different  $n$  are very similar. This is because the ADRC has the ability of rejecting a total disturbance that includes the modelling errors. Besides, the ADRC tuning equations (29) and (30) do not solely depend on the model order  $n$ , instead, it depend on  $nT$  together. This implies that when a process is modelled with different  $n$ , the value  $nT$  may not change significantly, considering that a

higher  $n$  usually results in a smaller  $T$  during identification, and vice versa. Thus, controller parameters and control results remain similar.

The above simulations also show the influence of measurement noise on the control input for three different control strategies. For ADRC control system, no additional filter is added but the variance of the noise on control input is still at acceptable level. This can be explained by analysing the transfer function from the noises  $n$  to the control input  $u$ ,  $G_{un}(s)$ .

$$G_{un}(s) = \frac{G_c F}{1 + G_c F G_p} = \frac{(B_2 s^2 + B_1 s + B_0)(Ts+1)^n}{b_0(s^3 + A_1 s^2 + A_0 s)(Ts+1)^n + (B_2 s^2 + B_1 s + B_0)K} \quad (40)$$

$$B_0 = k_p \beta_3, B_1 = k_p \beta_2 + k_d \beta_3, B_2 = k_p \beta_1 + k_d \beta_2 + \beta_3$$

$$A_0 = \beta_2 + k_d \beta_1 + k_p, A_1 = \beta_1 + k_d$$

The  $G_{un}(s)$  is strictly proper, implying that  $\lim_{\omega \rightarrow \infty} |G_{un}(i\omega)| = 0$ . Therefore, the high-frequency component of the measurement noise will decay and make limited influence on the control input. For MIGO tuning, the derivative term is not used, so the noise has little influence on the control input. While for PID control system,  $G_{un,PID}(s)$  is not proper, so the high frequency component of the noise will be magnified. Additional filter is necessary when high-frequency noise exists.

## V. EXPERIMENTAL VERIFICATION AND FIELD TEST

### D. Experimental tests on water tank

To validate the proposed ADRC tuning method, a laboratory test is performed on a water tank system. Fig. 7 shows the experiment setup. The water tank control system, developed by ©Feedback Instruments Ltd, consists of water tanks, pumps, sensors, a controller, and a monitor. In this experiment, water tanks 1 and 2 connected by a water tube are used. Water level  $y$  of Tank 2 is the process variable (PV), and the voltage of the pump  $u$  is the manipulated variable (MV).



Fig. 7. The water tank experiment setup

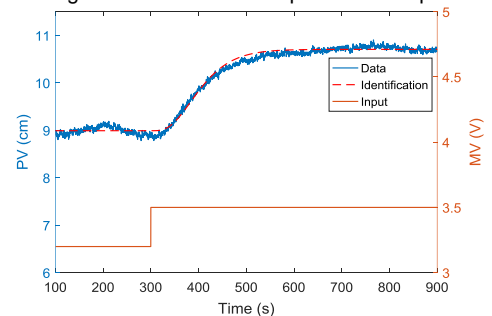


Fig. 8. Open loop step experimental data vs. Identified model

response

A step input is added in the open loop control system at the working point  $y=9$  cm, as shown in Fig. 8. Noted that the water level  $y$  is slightly oscillatory before a step input is added, but this does not influence the design of control system because the proposed ADRC tuning does not rely on accurate modelling. A rough high-order model is identified from the open loop system response data by using the empirical equations (35).

$$G \approx \frac{5.72}{(27.72s+1)^4} \quad (41)$$

For comparison purpose, PID algorithm is also implemented on the water tank. PID controller is tuned by the SIMC method due to its simplicity in use. The choice of  $\tau_c = \theta$  leads to the maximum sensitivity  $M_s = 1.4$  and the PID controller parameters are  $K_p = 0.1458$ ,  $K_i = 0.0021$ ,  $K_d = 2.4249$ . The tuning parameter of ADRC, the desired settling factor  $k = 4.17$ , is manually tuned to achieve the same maximum sensitivity of SIMC-PID, which gives the controller parameters  $\omega_c = 0.0278$ ,  $\omega_o = 0.2775$ ,  $b_0 = 0.0246$ .

These two controllers were tested by changing the water level set point from 9 cm to 11 cm first, then an input step disturbance  $d=1V$  is artificially added in the system at time  $t=1000$  s. Fig. 9 shows the real time control results. It can be seen that the proposed ADRC tuning results in slightly slower response during the set-point tracking,  $t=500-1000$  s, but ADRC has much better performance in disturbance rejection.

Moreover, the MV chattering under ADRC algorithm is less severe than SIMC-PID. Note that the calculated ADRC parameters are directly used on the plant without retuning. The experimental results demonstrate the reliability and effectiveness of the proposed ADRC tuning method.

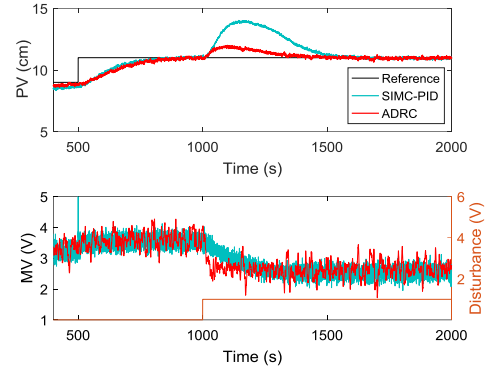


Fig. 9. Experiment results under SIMC-PID and proposed ADRC tuning parameters

Although it is expected that ADRC behaves better than SIMC-PID in terms of disturbance rejection, the ADRC results of the water tank experiment show much better disturbance rejection than the simulated situation. A possible reason is that the working condition has varied, such as water level change of the water reserve, change of pump characteristic, to the direction that is beneficial to ADRC control.

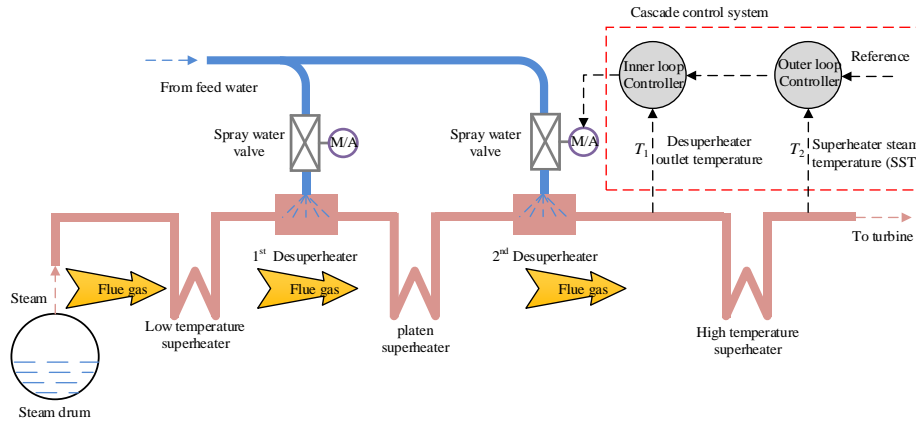


Fig. 10. The schematic diagram of the superheater steam temperature control system in CFB power plant

### E. Field tests on a power plant

Encouraged by the positive results from simulation examples and water tank experiment, the proposed ADRC tuning method is further applied to the superheater steam temperature (SST) control in a 330 MW in-service CFB unit in Shanxi, China. The SST control system, which is one of the most important control systems in the power plant, is a typical high-order process. The SST has to be controlled within a certain range, so that the temperature will not exceed the upper limit that is set for safe operation of the steam turbine. At the meantime, the temperature will not drop out of the lower limit that ensures the efficiency of the whole power plant. For this CFB unit, the allowable SST temperature fluctuation range is  $\pm 5$  °C. The steam that comes from the drum is heated by the fuel gas through three sets of superheaters as show in Fig. 10. Two sets

of desuperheaters are deployed to control the steam temperature. Since the control of the 2<sup>nd</sup> desuperheater directly influence the SST, ADRC control algorithm and the proposed tuning method are implemented on the 2<sup>nd</sup> desuperheater.

For the purpose of controller design, the SST models are identified from the open-loop data. As shown in Fig. 11, it is not a standard open-loop step test, because there is a spike in the control input signal and the control input changes before the temperature reaches steady state due to the operation limit. Therefore, the superheater models are identified by using optimization method instead of the empirical formulas presented in (35). The dynamic from the spray water valve to the desuperheater outlet temperature  $T_1$  is denoted as model  $G_1(s)$ , and the dynamic from the desuperheater outlet temperature  $T_1$  to the SST  $T_2$  is denoted as model  $G_2(s)$ .

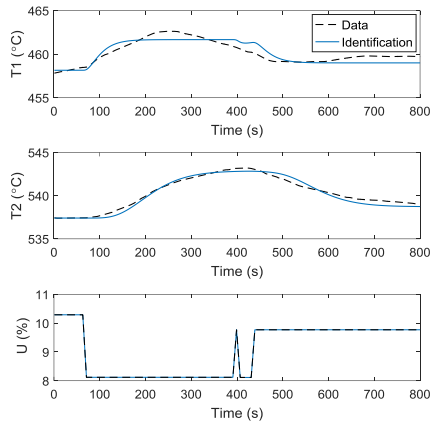


Fig. 11. Identification results of the superheater steam temperature control system

The model identification process is accomplished by MATLAB Simulink parameter estimation tool. The chosen optimization method is pattern search. The model order  $n$  is decided by choosing the identified model with the lowest cost function value. The identification results are shown in Fig. 11 and the identified transfer functions are

$$G_1(s) = \frac{-1.6165}{(19.363s+1)^2} \quad G_2(s) = \frac{1.5528}{(28.234s+1)^4}. \quad (42)$$

For the simplicity of implementing the control algorithm and relevant protective logics in the distributed control system (DCS), the first-order ADRC control algorithm is chosen to enhance the control performance of the SST control system. Compared to the outer loop process model  $G_2(s)$ , the inner loop process model  $G_1(s)$  is relatively fast response, and usually the PI controller or even the P controller is enough to eliminate the disturbances in the inner loop. Therefore, the inner PI controller remains unchanged and the first-order ADRC is implemented as outer loop controller in parallel with the original outer loop PID controller (see Fig. 12).

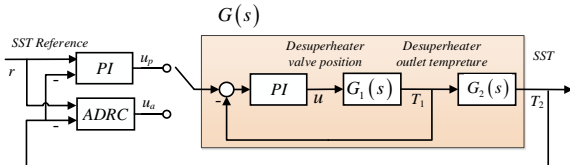


Fig. 12. Cascade control system of the superheater steam temperature

The tuning of the outer loop controller is based on the equivalent model  $G(s)$  for the combined inner controlled system and the model  $G_2(s)$ , as shown in Fig. 12. The inner PI controller parameters are  $K_{p2} = -1$ ,  $K_{i2} = -1/40$ , so the equivalent model for outer loop controller is

$$G(s) = \frac{G_{c,inner}(s)G_1(s)}{1 + G_{c,inner}(s)G_1(s)} G_2(s) \approx \frac{1.5528}{(27.4259s+1)^5}. \quad (43)$$

The outer loop PI is tuned by the experienced field engineer, and the PI parameters are  $K_{p1} = 1/3$ ,  $K_{i1} = 1/240$ , which results in a robustness level of  $M_s = 1.5$ . ADRC controller parameters are calculated by using (30). The desired settling time factor is manually tuned as  $k = 3.9$  to achieve a similar maximum sensitivity of SIMC-PI tuning, which gives ADRC control parameters  $\omega_c = 0.0187$ ,  $\omega_o = 0.187$ ,  $b_0 = 0.4554$ .

Two sets of field test results are shown in Fig. 13 and Fig. 14.

Fig. 13 shows the SST control result when the outer loop controller switches between PI and ADRC. Fig. 14 compares the control results under reference step change. It should be mentioned that the artificial input disturbance is not allowed for the commercial operation of the power plant, thus the strict disturbance rejection tests are not performed.

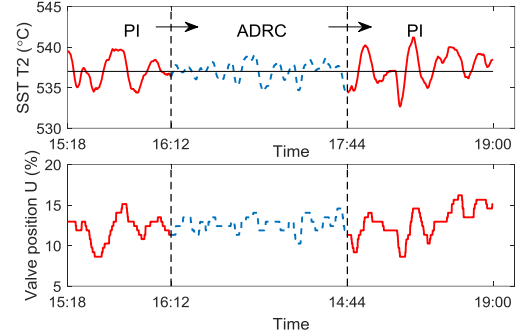


Fig. 13. Field test 1: switch between PI and ADRC with the SST set-point of 537°C (date of test: 15<sup>th</sup> of March, 2017)

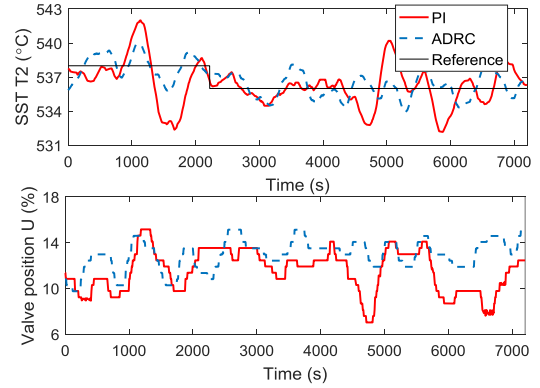


Fig. 14. Field test 2: SST set-point step from 538°C to 536°C (Time span of PI test: 14<sup>th</sup> of March, 2017 07:00-09:30; time span of ADRC test: 16<sup>th</sup> of March, 2017 11:00-13:30)

In addition, control performance indices such as peak positive error  $e^+$ , peak negative error  $e^-$ , standard deviation  $\sigma$ , integral absolute error (IAE) and the TV of control input, are summarized in Table II.

TABLE II  
PERFORMANCE INDICES FOR THE SST CONTROL TESTS

Test	Controller	$e^+ / ^\circ\text{C}$	$e^- / ^\circ\text{C}$	$\sigma$	IAE	TV
Test 1	PID	4.20	-4.34	1.82	8519	44.4
	ADRC	2.08	-2.59	1.05	4645	37.1
Test 2	PID	4.20	-5.63	1.93	9836	66.6
	ADRC	2.18	-2.25	1.38	6757	53.5

It can be found that the proposed ADRC tuning method reduced the peak error and standard deviation  $\sigma$  by about 50%. The IAE is reduced by more than 30%. The TV of the control input is decreased by about 20%, which means less overall tear and wear of valves, so the lifetime of valves can be prolonged and the maintenance cost is therefore reduced.

The field test results show that the proposed ADRC tuning method can reduce the SST fluctuation to a large extent. Since the SST is one of the main concerns when the power plant changes its load, the reduced SST fluctuation range indicates the possibility of large-scale load-varying operation, thus also indicates the potential of flexible operation of power plants to integrate more renewables into grid.

## VI. CONCLUSION

This paper describes the derivation of a quantitative tuning rule for low-order ADRC controller. In order to derive parameters under sensitivity constraint, an asymptote condition is propounded. Rooted from the high-order process system control, the proposed tuning rule has been expanded to other types of process applications. Comparative simulation studies, laboratory experiments and field tests have shown the efficiency of this tuning method. Future research will be continued on the ADRC parameters tuning toward multivariable processes.

## REFERENCES

- [1] H. Radim and R. Wagnerová, "Design and implementation of cascade control structure for superheated steam temperature control," in *Proc. Carpathian Control Conference (ICCC)*, 2016 17th International. IEEE, pp. 253-258.
- [2] L. Sun, et al., "Multi-objective optimization for advanced superheater steam temperature control in a 300 MW power plant," *Applied Energy*, vol. 208, pp. 592-606, 2017.
- [3] L. Sun, D. Li, K. Y. Lee and Y. Xue, "Control-oriented modeling and analysis of direct energy balance in coal-fired boiler-turbine unit," *Control Engineering Practice*, vol. 55, pp. 38-55, 2016.
- [4] L. Peng, D. Chen and C. Wang, "A high-order model for spike-type instability in axial compression systems," in *Proc. 2017 36<sup>th</sup> Chin. Control Conf.*, July 2017, pp. 21811-2185.
- [5] C. Ruth and K. Morris, "Transfer functions of distributed parameter systems: A tutorial," *Automatica*, vol. 45.5, pp. 1101-1116, 2009.
- [6] L. Sun, D. Li, and K. Y. Lee, "Optimal disturbance rejection for PI controller with constraints on relative delay margin," *ISA transactions*, vol. 63, pp. 103-111, Jul. 2016.
- [7] L. Guo and S. Cao, "Anti-disturbance control theory for systems with multiple disturbances: A survey," *ISA transactions*, vol. 53, pp. 846-849, 2014.
- [8] W. Chen, J. Yang, L. Guo and S. Li, "Disturbance-observer-based control and related methods—An overview," *IEEE Transactions on Industrial Electronics*, vol. 63, pp. 1083-1095, 2016.
- [9] J. Han, "Auto-disturbance rejection controller and its applications", *Control and Decision*, vol. 10, pp.85-88, 1998.
- [10] J. Han, "From PID to active disturbance rejection control," *IEEE Transactions on Industrial Electronics*, vol. 56, pp. 900-906, 2009.
- [11] H. Feng and B.Z. Guo, "Active disturbance rejection control: Old and new results," *Annual Reviews in Control*, vol. 44, pp. 226-237, 2017.
- [12] Z.L. Zhao and B.Z. Guo, "On convergence of nonlinear active disturbance rejection control for a class of nonlinear systems," *Journal of Dynamical and Control Systems*, vol. 22, pp. 385-412, 2016.
- [13] S. Shao and Z. Gao, "On the conditions of exponential stability in active disturbance rejection control based on singular perturbation analysis," *International Journal of Control*, vol. 90, pp. 2085-2097, 2017.
- [14] Y. Huang and W. Xue, "Active disturbance rejection control: methodology and theoretical analysis," *ISA transactions*, vol. 53, pp. 963-976, 2014.
- [15] L. Wang, Q. Li, C. Tong and Y. Yin, "Overview of active disturbance rejection control for systems with time-delay," *Control Theory & Applications*, vol. 30, pp. 1521-1533, 2013.
- [16] L. Sun, D. Li, Z. Gao, Y. Zhao, and S. Zhao, "Combined feedforward and model-assisted active disturbance rejection control for non-minimum phase system," *ISA transactions*, vol. 64, pp. 24-33, 2016.
- [17] S.N. Pawar and B.M. Patre, "Modified reduced order observer based linear active disturbance rejection control for TITO systems," *ISA transactions*, vol. 71, pp. 480-494, 2017.
- [18] L. Sun, J. Dong, D. Li and K.Y. Lee, "A practical multivariable control approach based on inverted decoupling and decentralized active disturbance rejection control," *Industrial & Engineering Chemistry Research*, vol. 55, no. 7, pp. 2008-2019, 2016.
- [19] Y. Xia, M. Fu, C. Li, F. Pu and Y. Xu, "Active disturbance rejection control for active suspension system of tracked vehicles with gun," *IEEE Transactions on Industrial Electronics*, vol. 65, no. 5, pp. 4051-4059, 2018.
- [20] Y. Su, C. Zheng and B. Duan, "Automatic disturbances rejection controller for precise motion control of permanent-magnet synchronous motors," *IEEE Transactions on Industrial Electronics*, vol. 52, no. 3, pp. 814-823, 2005.
- [21] Q. Zheng and Z. Gao, "An energy saving, factory-validated disturbance decoupling control design for extrusion processes," in *Intelligent Control and Automation (WCICA)*, 2012 10th World Congress on, IEEE, pp. 2891-2896.
- [22] S. Chen, Y. Zhang, D. Li and D. Lao, "ADRC decoupling controller design and parameters optimization for circulating fluidized bed boiler combustion system," in *Proc. 2013 32<sup>nd</sup> Chin. Control Conf.*, Xi'an, China, 2013, pp. 5504-5508. (in Chinese)
- [23] Z. Gao, "Scaling and bandwidth-parameterization based controller tuning," in *Proceedings of the American control conference*, vol. 6, pp. 4989-4996, 2006.
- [24] X. Chen, D. Li, Z. Gao and C. Wang, "Tuning method for second-order active disturbance rejection control," in *Proc. 2011 30<sup>th</sup> Chin. Control Conf.*, Yantai, China, 2011, pp. 6322-6327.
- [25] L. Wang, et al., "On control design and tuning for first order plus time delay plants with significant uncertainties," in *Proc. American Control Conference*, Chicago, USA, 2015. pp. 5276-5281.
- [26] K.J. Åström, H. Panagopoulos and T. Hägglund, "Design of PI controllers based on non-convex optimization," *Automatica*, vol. 34, no. 5, pp. 585-601, 1998.
- [27] Yaniv, O., and Nagurka, M., "Design of PID controllers satisfying gain margin and sensitivity constraints on a set of plants," *Automatica*, vol. 40, pp. 111-116, 2004.
- [28] C. Zhao and Y. Huang, "ADRC based input disturbance rejection for minimum-phase plants with unknown orders and/or uncertain relative degrees," *Journal of Systems Science and Complexity*, vol. 25, no. 4, pp. 625-640, 2012.
- [29] X. Yang, *Automatic control for thermal process*, 2nd ed., China: Tsinghua University Press, 2008. (in Chinese)
- [30] S. Skogestad, "Simple analytic rules for model reduction and PID controller tuning," *Journal of process control*, vol. 13, no. 4, pp. 291-309, 2003.
- [31] T. Hägglund and K.J. Åström, "Revisiting the Ziegler-Nichols tuning rules for PI control," *Asian Journal of Control*, vol. 4, no. 4, pp. 364-380, 2002.



**Ting He** received her B.S. degree in the School of Aerospace Engineering, Beijing Institute of Technology, in 2014. She is currently working on the Ph.D. degree in the Department of Energy and Power Engineering, Tsinghua University. Her research interests include active disturbance rejection control, process control, distributed energy system modelling, simulation and control.



**Zhenlong Wu** received the Bachelor's degree in thermal and power engineering from the School of Energy and Environment, Southeast University, Nanjing, China, in 2015. He is currently working toward the Ph.D. degree in the Department of Energy and Power Engineering, Tsinghua University, Beijing, China. He has authored several publications in the field of active disturbance rejection control and process control.



**Donghai Li** received his Ph.D. degree from Tsinghua University, Beijing, China, in 1994. He is currently an Associate Professor with the Department of Energy and Power Engineering, Tsinghua University. He has published more than 110 papers in control science, chaired or participated in more than 20 research projects. His research interests are PID control, active disturbance rejection control, hydrogenerator control, and gasifier control.



**Jihong Wang** (M'06–SM'12) received the Ph.D. degree from Coventry University, Coventry, U.K., in 1995. She is currently a Professor of Electrical Power and Control Engineering with the School of Engineering, University of Warwick, Coventry. Her current research interests include nonlinear system control, system modelling and identification, power systems, energy efficient actuators and systems, and applications of intelligent algorithms. Dr. Wang was a Technical Editor for the IEEE Transactions on Mechatronics.